Zhu et al. Aspects Nanotechnol 2018, 1(1):32-39
DOI: 10.36959/758/538 | Volume 1 | Issue 1

Aspects of Nanotechnology

Research Article Open Access

Targeting Ability of c(RGDyK)-Functionalized Nanoparticles is Inhibited by Protein Coronas

Shanshan Zhu[1], Yang Liu[2], Changhui Wang[2], Kai Ye[1], Ping Wang[1], Gang Huang[3] and Dannong He[1*]

[1]*National Engineering Research Center for Nanotechnology, Shanghai, China*

[2]*Shanghai Tenth People's Hospital, Shanghai, China*

[3]*Shanghai University of Medicine & Health Sciences, Shanghai, China*

Abstract

Nanoparticles functionalized with targeting ligands have been proposed as effective carriers for the selective delivery of diagnostic or therapeutic reagents to desired locations in the body. However protein coronas formed on the surface of such functionalized nanoparticles may affect their targeting efficiency when introduced into physiological environment. Here, Zinc Doped Iron Oxide Nanoparticles ($Zn_{0.4}Fe_{2.6}O_4$ NPs) were prepared, and functionalized with Cyclic arginine-glycine-aspartic Acid (c(RGDyK)) peptide to target U87MG cells. To investigate the effect of protein coronas on targeting efficiency, qualitative and quantitative approaches were utilized to compare the cellular uptake of nanoparticles pre-coated with or without bovine serum albumin (BSA). The results demonstrated that the specific particle-cell association was dramatically inhibited by protein coronas, indicating that the absorbed protein coronas could mask the targeting ligands on the surface of the nanoparticles and resulted in a considerable reduction in the functional targeting ability. This study provides novel insights into the significance of functionalized particles with a particular physiological environment.

Keywords

Cyclic RGD peptide, Magnetic nanoparticles, Protein corona, Targeting ability

Introduction

Particle-cell associations were extensively studied by numerous researchers in terms of corona formations on the nanoparticles surface [1-3]. Physicochemical properties of nanoparticles such as iron oxide [4], zinc oxide [5], titanium dioxide [6], silica [7] and gold [8] have been shown to profoundly influence the composition of the forming protein corona. And thus, the interactions of nanoparticles with cells and tissues are determined directly by this protein "corona" rather than the intrinsic properties of the nanoparticles [9]. From this point of view, the protein coronas could influence cellular uptake and trafficking of the nanoparticles [10] even with particle internalization, biodistribution and the clearance processes *in vivo* [11]. For instance, in order to deliver the nanoparticles to the binding target effectively, the nanoparticles were modified to avoid absorbing opsonization by phagocytes and detection by the immune system [12]. Surface modification of polymeric nanoparticles with poly(ethylene glycol) (PEG) has been proven to effectively reduce the absorption of opsonins, particularly IgG and complement [13]. Polysorbate 80-coated nanoparticles become spontaneously covered by dysopsonins such as apolipoproteins from the blood after injection, achieving long-circulating in the bloodstream and promoting nanoparticles to cross the blood-brain barrier [14]. In addition, the protein corona can also improve the therapeutic effect [15] and reduce the potential toxic effects of the high risk nanoparticles [16].

Targeting is an approach that can enhance the efficacy of cancer diagnosis and therapy by increasing the

***Corresponding authors:** Dannong He, National Engineering Research Center for Nanotechnology, Shanghai, 200241, China, Tel: 86-21-34291286-8035, E-mail: pingw2006@163.com

Received: December 11, 2017: **Accepted:** January 23, 2018: **Published online:** January 25, 2018

Citation: Zhu S, Liu Y, Wang C, et al. (2018) Targeting Ability of c(RGDyK)-Functionalized Nanoparticles is Inhibited by Protein Coronas. Aspects Nanotechnol 1(1):32-39

dose at the intended locations, thereby reducing the side effects in the bystander tissues [17]. Among the known approaches, active targeting is becoming increasingly prominent. Active targeting via specific ligands, such as proteins, antibodies or small biomolecules, can be recognized by the overexpressed receptors in the target cells [18]. Cyclic arginine-glycine-aspartic acid (c(RGDyK), y: tyrosine, K: lysine) peptides have been used to specifically bind to the overexpressed integrin $\alpha_v\beta_3$ on various tumor cells or on the tumor microvasculature [19-21]. Therefore, c(RGDyK) peptide was conjugated onto the ultrasmall superparamagnetic iron oxide nanocarriers to facilitate the uptake of the nanosystem by cancer cells such as glioblastomas [22,23].

However, when synthetic nanocarriers enter a particular biological milieu, protein coronas mentioned above may dictate the biological performance of the targeted nanoparticles *in vivo* by interfering with the targeting group [24]. Krais, et al. recently reported that targeted uptake of Fe_3O_4-SiO_2-FA (FA: folic acid) nanoparticles by ovarian cancer cells was observed only in the presence of serum [25]. Another study by Salvati, et al. provided the contrary result, showing that transferrin-functionalized nanoparticles lost their targeting capabilities for the reason that the adsorbed protein coronas could 'screen' targeting molecules on the surface of nanoparticles [26]. However, carbohydrate-based nanocarriers still exhibited high specific affinity for the binding of dendritic cells after incubation with plasma, suggesting that the targeting moieties remained accessible to the biological receptors despite the formation of a protein corona [27]. Therefore, these contradictory results suggest that more studies are needed to understand the potential effect of the protein coronas on targeting of nanoparticles.

According to our previous study, the synthesized $Zn_{0.4}Fe_{2.6}O_4$ nanoparticles (MNPs) own high saturation magnetization value and good biocompatibility [24]. In the present work, we intended to test whether the targeting ability of MNPs conjugated with c(RGDyK) would be affected by interacting with protein (Figure 1). To this end, Transmission Electron Microscope (TEM), Dynamic Light Scattering (DLS), zeta potential and cellular uptake studies before and after interactions with proteins were performed. In addition, the influence of the protein coronas on the targeting of U87MG human glioblastoma cells was also evaluated. Our results suggested that the absorbed protein layer could cover and deactivate the targeting group on the surfaces of MNPs.

Materials and Methods

Materials

The cyclic c(RGDyK) peptide (M_w = 706.8) was purchased from GenicBio BioTech Co. Ltd. (Shanghai, China). Oleylamine, 1-ethyl-3-[3-(dimethylamino)propyl] carbodiimide Hydrochloride (EDC), and N-hydroxysuccinimide (NHS) were supplied by J&K Chemical Ltd. (Shanghai, China). Cell counting kit-8 (CCK-8) was purchased from Beijing Fanbo Biochemicals Co., Ltd.

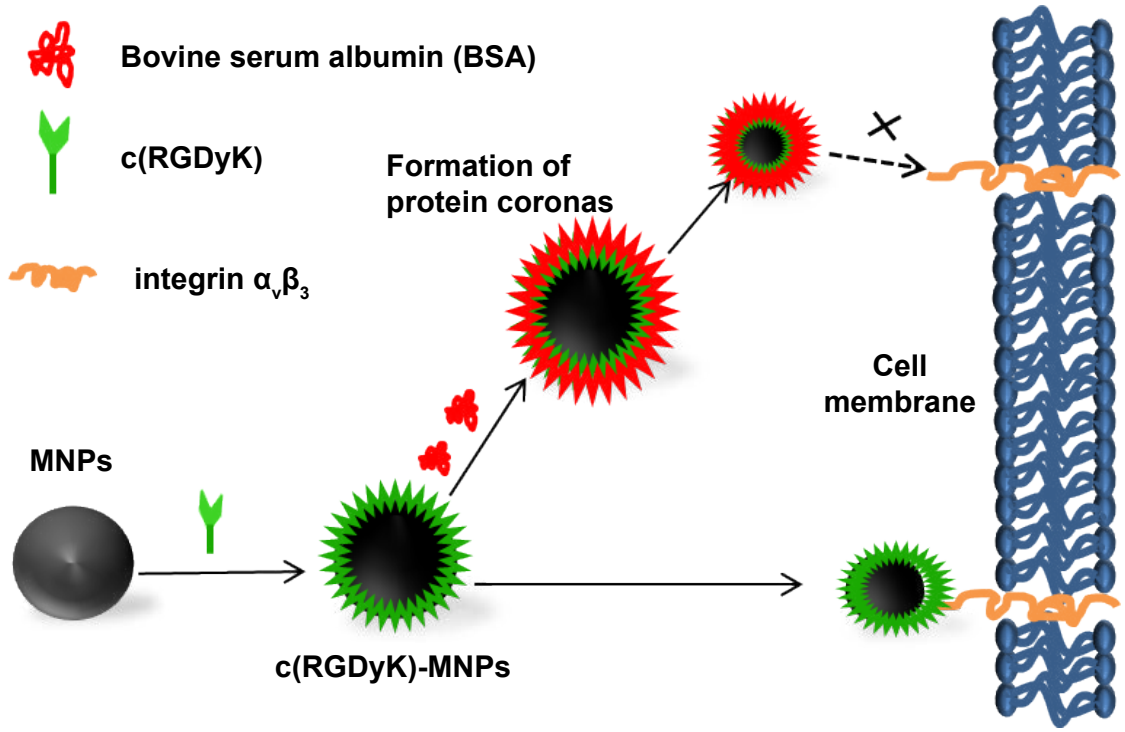

Figure 1: Schematic representation of the assembly of c(RGDyK)-MNPs, the formation of protein coronas in BSA solutions, and targeting of U87MG cells using nanoparticles with protein coronas formed on their surfaces.

All chemical reagents were analytical grade or above and purchased from Sinopharm Chemical Reagent Co., Ltd.

Conjugation of c(RGDyK) peptide to MNPs

The water-solube MNPs were synthesized following a previously reported method [28]. EDC (1 mg) and NHS (4 mg) were dissolved in 0.5 mL of phosphate buffered saline (PBS, 0.01M, pH 5.7), to which 1 mL of 5 mg/L MNPs aqueous solution was added. The reaction mixture was incubated vigorously with continuous stirring in the dark for 2 h at room temperature. Then, 0.5 mL of 2 mg mL^{-1} c(RGDyK) were poured into the solution of activated MNPs, and the mixture was incubated overnight at room temperature in the dark with continuous stirring. The formed c(RGDyK)-MNPs were collected by a permanent magnet to remove the unreacted c(RGDyK) and then redispersed in PBS at 4 °C for further application.

Incubation of nanoparticles with human plasma

All experiments were conducted at least twice to ensure reproducibility. Nanoparticles (5 mg/mL) were incubated with bovine serum albumin (BSA) at a constant concentration of 20 mg/mL for 1 h at 37 °C with shaking at 150 rpm. After that, the nanoparticle-protein complexes were then collected by a permanent magnet and washed three times with PBS to obtain the "hard" protein corona-coated particles. Then, the nanoparticle-protein complexes were resuspended in MilliQ water and characterized with the help of TEM (JEOL, JEM-2100F, Tokyo, Japan), and Zetasizer Nano (Malvern, Worcestershire, UK).

Cell culture

The U87MG human glioblastoma cell line was kindly donated by Prof. Weiyue Lu (School of Pharmacy, Fudan University, Shanghai, China). Cells were maintained as monolayer cultures at 37 °C in 5% CO_2 atmosphere in high-glucose Dulbecco's Modified Eagle Medium (DMEM, Gibco) supplemented with 10% Fetal Bovine Serum (FBS, Gibco), and 1% penicillin/streptomycin (HyClone).

Cell viability assessment

The cytotoxicities of all nanoparticles for U87MG cells were tested using a CCK-8 kit (CCK-8 Kit, Boya Biotech, Beijing, China) [29]. U87MG cells were seeded in 96-well culture plates and incubated in DMEM medium for 24 h. The cells were washed with three times with warm PBS and then incubated with 200 μL of FBS-free medium containing various equivalent concentrations of nanoparticles for 24 h. Cells were washed gently with PBS and cytotoxicity assay was performed using CCK-8 Kits following the manufacturer's instructions.

Confocal microscopic imaging

U87MG cells (1×10^6 cells per mL) were seeded in 4-well culture plates with glass bottom and incubated for 12 h. The medium was replaced with FBS-free medium containing 100 μg/mL nanoparticles and incubated for 3 h. After that, cells were washed three times with PBS, fixed with 4% paraformaldehyde for 30 min and stained by 2 μg/mL 4',6-diamidino-2-phenylindole (DAPI, Life Tech, Grand Island, NY) for 8 min. Images of these fluorescently stained cells were then captured using a confocal laser scanning microscope (CLSM, Leica, TCS SP5, Mannheim, Germany).

Cellular uptake study

For quantitative analysis of the cellular uptake of nanoparticles, U87MG cells were seeded in six-well plates (Costar, Charlotte, NC) and cultured in DMEM overnight. Then cells were washed with PBS for three times and FBS-free media containing various types of nanoparticles (50 μg/mL) were added into each well, followed by 24 h of co-incubation. At determined time points, cells were washed for four times with PBS. To determine the Fe contents in cells by inductively coupled plasma optical emission spectroscope (ICP-OES, 710, Varian, USA) the cells were collected and digested with 50 mM NaOH solution. Each test was run with three samples in parallel.

Statistical analysis

Each result is presented as mean ± standard deviation (SD). Statistical significance in the differences between different groups was evaluated by LSD *t*-tests or Tukey's method after analysis of variance (ANOVA). Differences were considered statistically significant at $p < 0.05$.

Result and Discussion

Figure 2 presents the X-Ray diffraction (XRD) pattern of as obtained MNPs, which matches well with

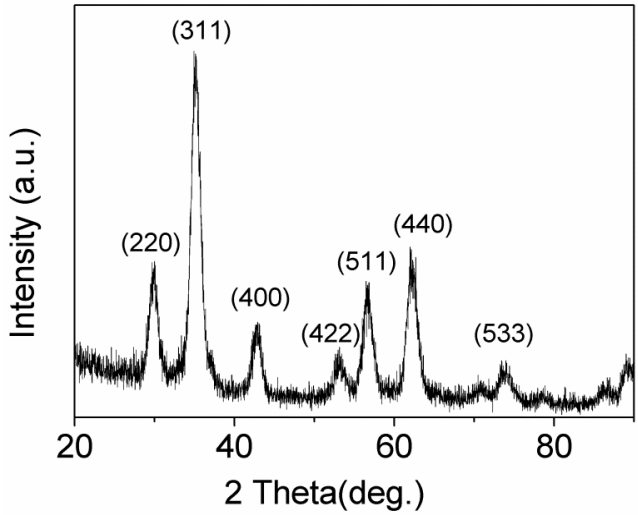

Figure 2: X-ray diffraction pattern of MNPs.

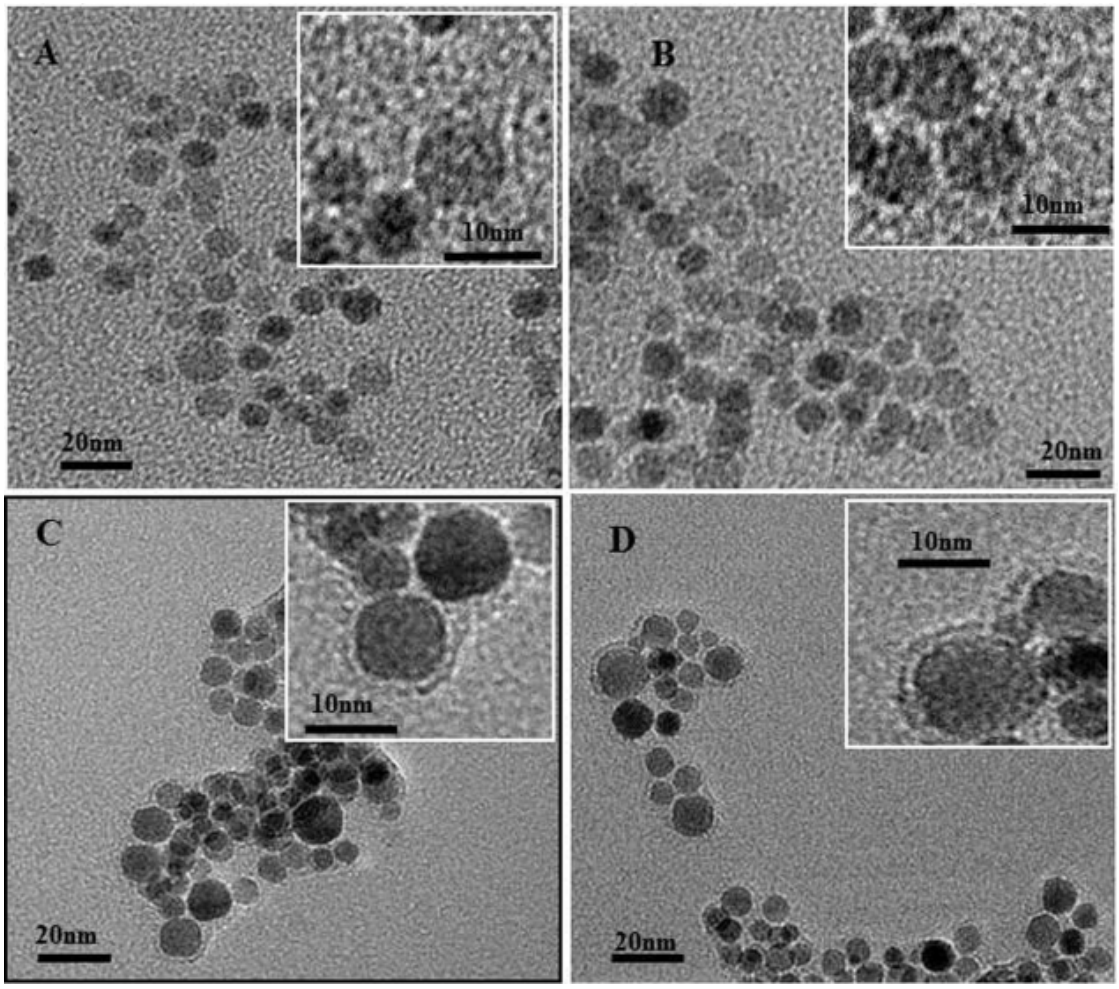

Figure 3: TEM images of nanoparticles A) MNPs; B) c(RGDyK)-MNPs; C) MNPs with protein coronas; D) c(RGDyK)-MNPs with protein coronas.

Table 1: Hydrodynamic diameter (A) or zeta potential (B) of the nanoparticles without the protein corona or with the protein coronas by incubating with BSA for 1 h. Significant difference vs in water group ($^{*}p < 0.01$).

(A)

	MNPs		c(RGDyK)-MNPs	
DLS (nm)	Water	BSA	Water	BSA
0 h	112.4 ± 4.9	112.4 ± 4.9	118.5 ± 7.6	118.5 ± 7.6
1 h	121.0 ± 4.7	156.6 ± 3.8*	112.7 ± 3.9	239.4 ± 1.9*

(B)

Zeta potential (mV)	MNPs		c(RGDyK)-MNPs	
	Water	BSA	Water	BSA
0 h	-20.4 ± 1.3	-20.4 ± 1.3	-30.4 ± 1.3	-30.4 ± 1.3
1 h	-20.7 ± 1.0	-14.3 ± 0.9*	-30.7 ± 1.0	-15.7 ± 1.4*

the standard powder diffraction data for bulk cubic spinel-structured magnetite (JCPDS file no. 75-0033). C(RGDyK) as a targeting ligand was successfully covalently immobilized onto carboxyl-modified MNPs by the use of EDC and NHS, which was confirmed by DLS (Table 1A) and zeta potential (Table 1B). The mean hydrodynamic size of c(RGDyK)-MNPs (118.5 ± 7.6 nm) was not obviously altered compared to that of MNPs (112.4 ± 4.9 nm). However, due to the negative charge of aspartic acids in the c(RGDyK) peptides [30], c(RGDyK)-MNPs exhibited a decrease in zeta-potential (-30.4 ± 1.3 mV) compared to that of MNPs (-20.4 ± 1.3). These results indicated that surface functional groups on MNPs were altered, in other words, the conjugation of MNPs with c(RGDyK) was successful.

Surface protein adsorption on nanoparticles was analysed by DLS, zeta potential and TEM after incubation with BSA for 1 h. For both MNPs and c(RGDyK)-MNPs, the formation of protein coronas resulted in an increase in particle size and a slight change in the ζ-potential. Specifically, the zeta-potential of nanoparticles showed the change from -20.4 ± 1.3 mV (MNPs), -30.4 ± 1.3 mV (c(RGDyK)-MNPs) in the absence of a protein corona, to -14.3 ± 0.9 mV and -15.7 ± 1.4 mV in the presence of protein coronas, with a corresponding variation in size from 112.4 ± 4.9 nm, 118.5 ± 7.6 nm to 156.6 ± 3.8 nm (1.4-fold), 239.4 ± 1.9 nm (2-fold increase). The change in the ζ-potential is consistent with the previous study, which demonstrated that adsorption of proteins at various concentrations significantly neutralized the surface

charge of the particles [31]. Furthermore, TEM was employed to examine the surface morphology of the MNPs and c(RGDyK)-MNPs in the presence of protein coronas. The protein coating layers were clearly observed by TEM for both of nanoparticles after adsorption of proteins onto the surfaces (Figure 3).

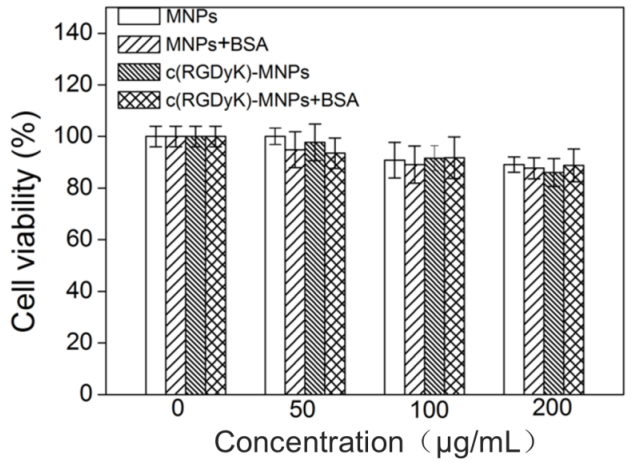

Figure 4: Cell viability assessment of nanoparticles in the presence/absence BSA. Cell viability of nanoparticles was assessed on U87MG cells using the CCK assay. U87MG cells were exposed to different concentrations of nanoparticles in FBS-free DMEM for 24 h. Results are presented as mean values ± SDs (n = 3). The average cell viability of the control group is set as 100%, and the cell viability of other groups is normalized to the control group.

Cytotoxicity of all nanoparticle formulations was evaluated on U87MG tumor cells using CCK-8 assay in FBS-free DMEM. No significant differences in cell viability for any type of nanoparticles after 1 day of incubation were observed within the given concentration range (Figure 4). The results suggested that the developed nanoparticles exhibited excellent cytocompatibility in the absence or presence of protein.

Cell viability of nanoparticles was assessed on U87MG cells using the CCK assay. U87MG cells were exposed to different concentrations of nanoparticles in FBS-free DMEM for 24 h. Results are presented as mean values ± SDs (n = 3). The average cell viability of the control group is set as 100%, and the cell viability of other groups is normalized to the control group.

To qualitatively examine the cellular uptake behaviors of the nanocarriers in the absence/presence of BSA, U87MG glioblastoma cells were incubated with MNPs, MNPs + BSA, c(RGDyK)-MNPs and c(RGDyK)-MNPs + BSA for 3 h, conducted with fluorescent staining, and

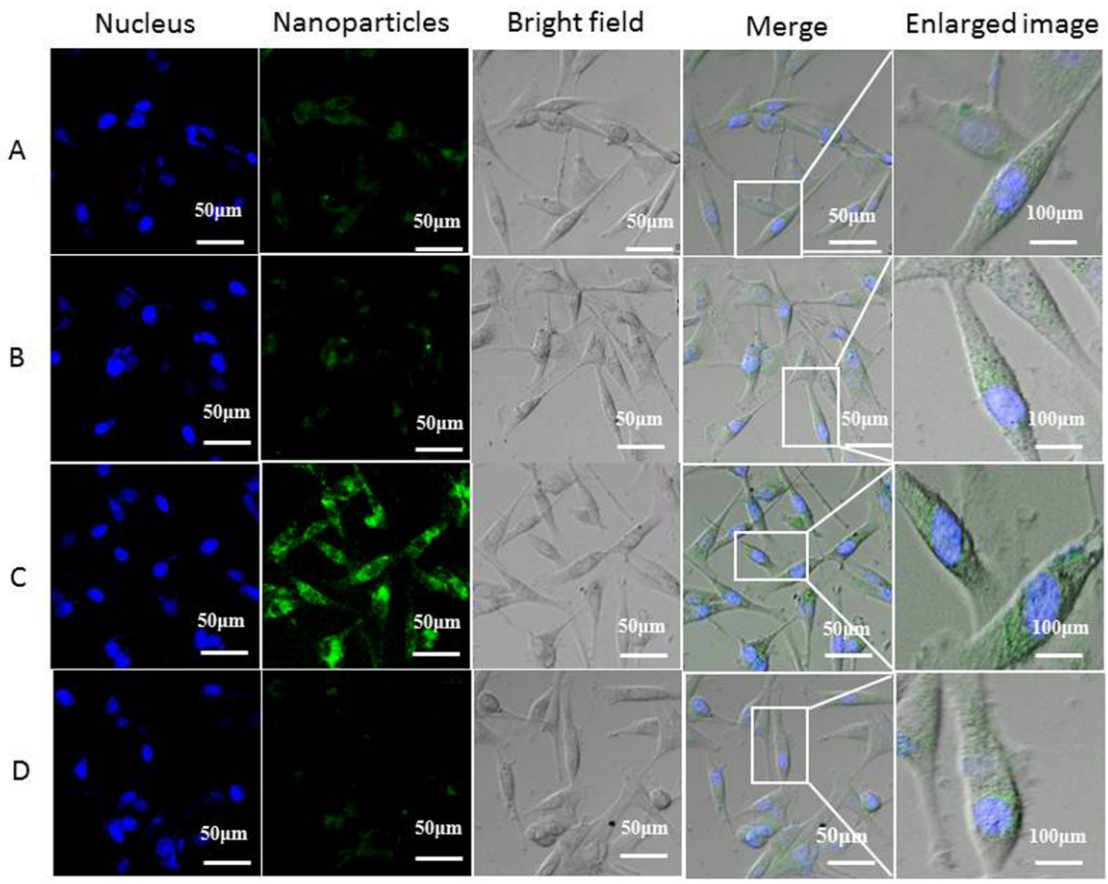

Figure 5: Confocal microscopic imaging of U87MG cells incubated with nanoparticles in the presence/absence BSA A) MNPs without a protein corona; B) MNPs with a protein corona; C) c(RGDyK)-MNPs without a protein corona; D) c(RGDyK)-MNPs with a protein corona. Blue: DAPI-stained nuclei; green: FITC-conjugated MNPs and c(RGDyK)-MNP.

observed with a CLSM (Figure 5). To enable the visualization of the uptake of the nanocarriers under the microscope, fluorescein isothiocyanate (FITC) was conjugated to the nanoparticles as a tracker. As expected, the higher fluorescence intensity could be visualized in U87MG cells treated with c(RGDyK)-MNPs compared to those treated with MNPs, namely that c(RGDyK) conjugation markedly facilitated the cellular uptake of c(RGDyK)-MNPs by U87MG cells. Interestingly, with a BSA coating, these cells treated with MNPs exhibited no significant difference in fluorescence, while an obvious decrease in fluorescence was observed in U87MG cells incubated with c(RGDyK)-MNPs. These results preliminarily proved that protein coronas might lead to the loss of targeting ability of the functionalized particles.

We further investigated the effect of protein coronas on the specific targeting ability of c(RGDyK)-MNPs by quantitatively analysing the intracellular Fe content by ICP-OES after incubation with U87MG cells for 3 h and 6 h. As shown in Figure 6, the amount of the internalized iron increased with the incubation time for any type of nanoparticles. In addition, the c(RGDyK) modification significantly enhanced the cellular uptake by U87MG cells compared with MNPs in the absence of BSA. The BSA significantly decreased the cellular uptake of c(RGDyK)-MNPs regardless of the incubation time, whereas almost no noticeable difference was observed in the cellular uptake of MNPs with or without BSA. These results implied that the targeting capacity of c(RGDyK)-MNPs was lost when they interacted with BSA and formed a protein corona.

Quantitative intracellular uptake of iron ion by U87MG cells without or with a BSA coating as a function of incubation time. Results are presented as means ± SDs (n = 3). Statistical analysis of the differences in uptake was performed using Student's t-tests ($^*P < 0.01$).

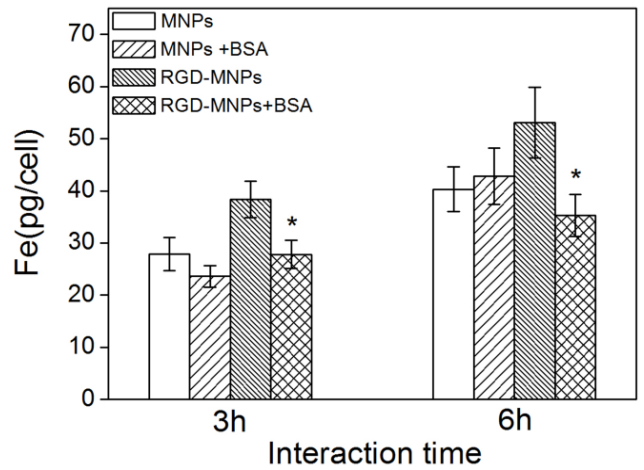

Figure 6: ICP-OES analysis of the Fe content in U87MG cell. Quantitative intracellular uptake of iron ion by U87MG cells without or with a BSA coating as a function of incubation time. Results are presented as means ± SDs (n = 3). Statistical analysis of the differences in uptake was performed using Student's t-tests ($^*P < 0.01$).

Here, we exploited the c(RGDyK)-conjugated MNPs to target U87MG cells expressing high levels of integrin $\alpha_v\beta_3$. A previous study has demonstrated specific binding of c(RGDyK)-Fe_3O_4 to integrin $\alpha_v\beta_3$ in tumor neo-vessels, which is able to provide a reliable biomarker of intact tumor in therapeutic trials [22]. For instance, c(RGDyK)-Fe_3O_4 as a contrast agent for magnetic resonance imaging (MRI) can target glioblastoma by binding to integrin $\alpha_v\beta_3$, and show higher sensitivity in *in vivo* noninvasive monitoring of early tumor responses to antiangiogenic therapies [32]. Moreover, the Dox-loaded c(RGDyK)-conjugated superparamagnetic iron oxide (SPIO) particles are capable of being therapeutic agents and MRI contrast agents simultaneously because of their preferential binding towards U87MG cells [30]. In our study, by combining CLSM and ICP-OES analysis which allows qualitative and quantitative determination of the cellular uptake of these nanoparticles, we proved that c(RGDyK) indeed favored selective uptake of MNPs into U87MG cells. As for the MNPs with protein coronas derived from BSA solutions, no noticeable differences in cellular uptake were observed compared with MNPs without protein coronas. This result was consistent with a previous finding, which reported that the absorbed protein coronas on the poly(methacrylic acid)-naked particles did not significantly alter the association with SK-OV-3 cells [31]. In most cases, the uptake of particles decreases in the presence of a protein coating [33,34]. On the contrary, the formation of a tunable protein corona has been shown to increase targeting efficiency, thereby enhancing cellular internalization [35,36]. This discrepancy may be comprehensible, as the physicochemical properties of nanoparticles (i.e., size, composition, shape, and surface chemistry) determine the corona's composition, which influences the particle-cell interactions [37].

A dramatically decreased cellular uptake of c(RGDyK)-MNPs was observed in the presence of BSA than that in the absence of BSA. The result implied that the absorbed protein corona led to the loss of targeting ability of c(RGDyK)-MNPs. A potential reason for the limited specificity in targeting is the masking of conjugated targeting ligands in the presence of BSA solutions, namely, the absorbed protein corona impairs the ligand-receptor interactions, thereby reducing particle-cell interactions for the c(RGDyK)-functionalized particles. It has been reported that PEGylation may mask or change the orientation of targeting ligands besides reducing protein binding [38]. Furthermore, one study demonstrated that the decreased targeting capability was correlated to the increased PEG density on nanoparticles [39]. Another

factor which has been reported to influence the cellular interactions with particles is the neutralization of surface charge by the absorbed protein corona [40]. Based on our DLS analysis, the negative zeta potentials of the c(RGDyK)-MNPs were reduced with a BSA coating. This result might afford to be part of the reason for which the formed protein corona decreased the uptake efficacy of c(RGDyK)-MNPs by U87MG cells. Although, compared with c(RGDyK)-MNPs, the zeta potential of the MNPs exhibited similar level of change after incubation with BSA, the uptake of the particles was shown to have no difference. Therefore, the decreased targeting efficiency of c(RGDyK)-MNPs after protein adsorption could not be explained by the differences in the surface charge. This matches the results published previously, which reported that two folic acid-functionalized nanoparticles with similar zeta potentials showed difference in specific uptake in the presence of serum, indicating that the discrepant effects on targeting capability could not be attributed to the surface charge [25]. However, the above discussion can't thoroughly elucidate the current observation that specific (c(RGDyK)-mediated) uptake was reduced in the presence of serum. Further studies are desired to investigate the effect of serum proteins on targeting ability and the underlying potential mechanisms.

Conclusion

We have developed c(RGDyK)-functionalized magnetic nanoparticles, and examined the effect of protein coronas on the targeting ability of c(RGDyK)-MNPs. Our results showed that the formation of protein coronas led to changes in the zeta potential of the functionalized particles. The nanoparticles were noncytotoxic for U87MG cells whether in the presence or absence of proteins. More significantly, c(RGDyK)-MNPs were specifically internalized in a c(RGDyK) receptor-dependent manner, whereas the adsorption of protein decreased the overall uptake dramatically, suggesting that the c(RGDyK)-MNPs might lose their targeting ability owing to the protein coronas. In summary, this study demonstrated that the targeting specificity of functionalized particles could be changed upon exposure to protein. Therefore, it seems imperative to carry out more detailed studies *in vitro* firstly to guarantee the targeting ability of the functionalized particles before *in vivo* application. In addition, further studies are proposed to focus on how to design the nanoparticles which are able to retain or even enhance their targeting ability in the presence of a particular physiological environment by regulating the surface properties of the particles.

Acknowledgment

This work was supported by the National Basic Research Program of China (2013CB932500), the Shanghai Rising-Star Program (15QB1402200), China National Science Funds for Young Scholars (21403156).

References

1. S Tenzer, D Docter, J Kuharev, et al. (2013) Rapid formation of plasma protein corona critically affects nanoparticle pathophysiology. Nature Nanotechnology 8: 772-781.
2. M Lundqvist, J Stigler, G Elia, et al. (2008) Nanoparticle size and surface properties determine the protein corona with possible implications for biological impacts. Proc Natl Acad Sci U S A 105: 14265-14270.
3. E Casals, T Pfaller, A Duschl, et al. (2010) Time evolution of the nanoparticle protein corona. ACS Nano 4: 3623-3632.
4. T Zhao, K Chen, H Gu (2013) Investigations on the interactions of proteins with polyampholyte-coated magnetite nanoparticles. J Phys Chem B 117: 14129-14135.
5. IL Hsiao, YJ Huang (2013) Effects of serum on cytotoxicity of nano- and micro-sized ZnO particles. J Nanopart Res 15: 1829-1845.
6. R Tedja, M Lim, R Amal, et al. (2012) Effects of serum adsorption on cellular uptake profile and consequent impact of titanium dioxide nanoparticles on human lung cell lines. ACS Nano 6: 4083-4093.
7. E Izak-Nau, M Voetz, S Eiden, et al. (2013) Altered characteristics of silica nanoparticles in bovine and human serum: the importance of nanomaterial characterization prior to its toxicological evaluation. Part Fibre Toxicol 10: 56.
8. S Dominguez-Medina, S McDonough, P Swanglap, et al. (2012) In situ measurement of bovine serum albumin interaction with gold nanospheres. Langmuir 28: 9131-9139.
9. F Klemm, R Johnson, VM Mirsky (2015) Binding of protein nanoparticles to immobilized receptors. Sensors and Actuators B: Chemical 208: 616-621.
10. BD Chithrani, WC Chan (2007) Elucidating the mechanism of cellular uptake and removal of protein-coated gold nanoparticles of different sizes and shapes. Nano Lett 7: 1542-1550.
11. SR Saptarshi, A Duschl, AL Lopata (2013) Interaction of nanoparticles with proteins: relation to bio-reactivity of the nanoparticles. Journal of Nanobiotechnology 11: 1-12.
12. SD Li, L Huang (2010) Stealth nanoparticles: High density but sheddable PEG is a key for tumor targeting. J Control Release 145: 178-181.
13. AS Karakoti, S Das, S Thevuthasan, et al. (2011) PEGylated inorganic nanoparticles. Angew Chem Int Ed Engl 50: 1980-1994.
14. J Kreuter, D Shamenkov, V Petrov, et al. (2002) Apolipoprotein-mediated transport of nanoparticle-bound drugs across the blood-brain barrier. J Drug Target 10: 317-325.
15. MJ Hajipour, O Akhavan, A Meidanchi, et al. (2014) Hyperthermia-induced protein corona improves the therapeutic effects of zinc ferrite spinel-graphene sheets against cancer. RSC Adv 4: 62557-62565.
16. DA Mbeh, O Akhavan, T Javanbakht, et al. (2014) Cytotoxicity of protein corona-graphene oxide nanoribbons on human epithelial cells. Applied Surface Science 320: 596-601.
17. AM Nystrom, B Fadeel (2012) Safety assessment of nano-

materials: Implications for nanomedicine. J Control Release 161: 403-408.

18. ME Davis, JE Zuckerman, CH Choi, et al. (2010) Evidence of RNAi in humans from systemically administered siRNA via targeted nanoparticles. Nature 464: 1067-1070.
19. Y Li, Y Zhao, W Chan, et al. (2015) Selective tracking of lysosomal Cu2+ ions using simultaneous target- and location-activated fluorescent nanoprobes. Anal Chem 87: 584-591.
20. Akhavan, E Ghaderi, H Emamy (2012) Nontoxic concentrations of PEGylated graphene nanoribbons for selective cancer cell imaging and photothermal therapy. J Mater Chem 22: 20626-20633.
21. JT Robinson, SM Tabakman, YY Liang, et al. (2011) Ultrasmall reduced graphene oxide with high near-infrared absorbance for photothermal therapy. J Am Chem Soc 133: 6825-6831.
22. S Melemenidis, A Jefferson, N Ruparelia, et al. (2015) Molecular magnetic resonance imaging of angiogenesis in vivo using polyvalent cyclic RGD-iron oxide microparticle conjugates. Theranostics 5: 515-529.
23. J Xie, K Chen, HY Lee, et al. (2008) Ultrasmall c(RGDyK)-coated Fe3O4 nanoparticles and their specific targeting to integrin alpha(v)beta3-rich tumor cells. J Am Chem Soc 130: 7542-7543.
24. E Mahon, A Salvati, F Baldelli Bombelli, et al. (2012) Designing the nanoparticle-biomolecule interface for "targeting and therapeutic delivery". J Control Release 161: 164-174.
25. A Krais, L Wortmann, L Hermanns, et al. (2014) Targeted uptake of folic acid-functionalized iron oxide nanoparticles by ovarian cancer cells in the presence but not in the absence of serum. Nanomedicine 10: 1421-1431.
26. A Salvati, AS Pitek, MP Monopoli, et al. (2013) Transferrin-functionalized nanoparticles lose their targeting capabilities when a biomolecule corona adsorbs on the surface. Nature Nanotechnology 8: 137-143.
27. B Kang, PO kwieka, S Schottler, et al. (2015) Carbohydrate-based nanocarriers exhibiting specific cell targeting with minimum influence from the protein corona. Angew Chem Int Ed Engl 54: 7436-7440.
28. X Xu, SS Zhu, R Rong, et al. (2016) Evaluation of zinc-doped magnetite nanoparticle toxicity in the liver and kidney of mice after sub-chronic intragastric administration. Toxicology Research 5: 97-106.
29. H Tominaga, M Ishiyama, F Ohseto, et al. (1999) A Water-soluble tetrazolium salt useful for colorimetric cell viability assay. Anal Commun 36: 47-50.
30. MK Yu, J Park, YY Jeong, et al. (2010) Integrin-targeting thermally cross-linked superparamagnetic iron oxide nanoparticles for combined cancer imaging and drug delivery. Nanotechnology 21: 415102.
31. Q Dai, Y Yan, JL Guo, et al. (2015) Targeting ability of affibody-functionalized particles is enhanced by albumin but inhibited by serum coronas. ACS Macro Lett 4: 1259-1263.
32. F Zhang, X Huang, L Zhu, et al. (2012) Noninvasive monitoring of orthotopic glioblastoma therapy response using RGD-conjugated iron oxide nanoparticles. Biomaterials 33: 5414-5422.
33. G Baier, C Costa, A Zeller, et al. (2011) BSA adsorption on differently charged polystyrene nanoparticles using isothermal titration calorimetry and the influence on cellular uptake. Macromol Biosci 11: 628-638.
34. A Lesniak, F Fenaroli, MP Monopoli, et al. (2012) Effects of the presence or absence of a protein corona on silica nanoparticle uptake and impact on cells. ACS Nano 6: 5845-5857.
35. M Schäffler, F Sousa, A Wenk, et al. (2014) Blood protein coating of gold nanoparticles as potential tool for organ targeting. Biomaterials 35: 3455-3466.
36. D Bargheer, J Nielsen, G Gébel, et al. (2015) The fate of a designed protein corona on nanoparticles in vitro and in vivo. Beilstein J Nanotechnol 6: 36-46.
37. P Foroozandeh, AA Aziz (2015) Merging worlds of nanomaterials and biological environment_factors governing protein corona formation on nanoparticles and its biological consequences. Nanoscale Res Lett 10: 221.
38. DB Kirpotin, DC Drummond, Y Shao, et al. (2006) Antibody targeting of long-circulating lipidic nanoparticles does not increase tumor localization but does increase internalization in animal models. Cancer Res 66: 6732-6740.
39. S Hak, E Helgesen, HH Hektoen, et al. (2012) The effect of nanoparticle polyethylene glycol surface density on ligand-directed tumor targeting studied in vivo by dual modality imaging. ACS Nano 6: 5648-5658.
40. V Mirshafiee, R Kim, S Park, et al. (2016) Impact of protein pre-coating on the protein corona composition and nanoparticle cellular uptake. Biomaterials 75: 295-304.

DOI: 10.36959/758/538 | Volume 1 | Issue 1